Journal of Statistical Physics, Vol. 94, Nos. 3/4, 1999

Recurrence Times in Quasi-Periodic Motion: Statistical Properties, Role of Cell Size, Parameter Dependence

M. Theunissen,[1,2] C. Nicolis,[2] and G. Nicolis[1]

Received August 12, 1997; final September 14, 1998

We investigate the probabilistic properties of recurrence times for the simplest form of aperiodic deterministic dynamics, quasi-periodic motion. Previous results using number theory techniques predict two fundamental recurrence times for uniform quasi-periodic motion on a two-dimensional torus, while no analogous analytic result seems to exist for higher dimensional tori. The two-dimensional uniform case is reanalyzed from a more geometric point of view and new, workable expressions are derived that enable us fully to understand and predict the recurrence phenomenon and to analyze its parameter dependence. Emphasis is placed on the statistical properties and, in particular, on the variability of recurrence times around their mean, in relation to local Farey tree structure. Higher-dimensional tori are considered, and seen to also display a high variability in their finite-time recurrence behavior. The results are finally extended to the non-uniform quasi-periodic case.

KEY WORDS: Recurrence times; quasi-periodic motion; circle map; Farey tree; Diophantine approximation; Denjoy's theorem.

1. INTRODUCTION

There is an ongoing interest in the properties of recurrence times of deterministic dynamical systems,[1–4] stimulated both by the historical importance of the early contributions by Poincaré and by the relevance of the subject in the foundations of statistical mechanics.[5]

[1] Center for Nonlinear Phenomena and Complex Systems, B-1050 Brussels, Belgium; e-mail: mtheunis@ulb.ac.be, gnicolis@ulb.ac.be.

[2] Institut Royal Météorologique de Belgique, 1180 Brussels, Belgium; e-mail: cnicolis@oma.be.

0022-4715/99/0200-0437$16.00/0

Recently, the statistics of recurrence times has been taken up as a tool toward the improvement of prediction techniques.[6–8] Indeed, consider a dynamical system, and let the corresponding (full or reduced) phase space be partitioned into cells. The investigation of the dynamics of transitions between the cells of this partition provides then one with considerable insight on the underlying fine scale dynamics and, in particular, its degree of predictability, since it gives information on the time delay between two successive passages of the trajectory in the "state" corresponding to the particular phase space cell considered.

Ordinarily, investigations on recurrence dynamics in the physical literature are limited to the evaluation of mean recurrence times. One may argue that, in many instances, this type of information is not sufficiently representative. On the one side, fluctuations around the mean are likely to be comparable to the mean itself since there is here no obvious argument analogous to the one penalizing the fluctuations of intensive thermodynamic quantities. And on the other side, since the dynamics is generally highly non-uniform as one moves across phase space, one expects to encounter a pronounced variability along the invariant manifold on which the trajectories are evolving. The investigation of the dynamical and statistical properties of recurrence times in quasi-periodic motion accounting for these two aspects is one of the principal objective of this work. The role of the parameters of the underlying system and of the size and shape of the phase space cell chosen will also be assessed. Numerical investigations will also be carried out and will help shedding light into the high complexity of the recurrence phenomenon.

Recurrence times in quasi-periodic motion have also attracted considerable attention in the mathematical literature. The main result in this area[9–11] is that the set of integers n such that $\{n\alpha\} = n\alpha \bmod 1$ is limited to an interval $[0, a)$, $a < 1$, displays gaps taking 2 or 3 different values, the third one being the sum of the first two. Lohöfer and Mayer[12] extended this result to more general intervals and gave expressions for these gaps, interpreted as the discrete recurrence times of an underlying two-dimensional quasiperiodic motion.

The generalization of these results to n-dimensional ($n > 2$) quasi-periodic motion seems to be largely open. Numerical evidence[13] indicates the persistence of n fundamental gaps or recurrence times, from which all other observed recurrence times (in finite number) are obtained as integer-valued combinations. An expression for the mean recurrence time in n-dimensional harmonic motion was also derived by Hemmer *et al.*[2] using a rather involved method.

In the present paper these results are first reformulated and rederived in a simple manner combining geometric and number theoretic arguments, more suitable for our further analysis of the probabilistic properties and the cell size and parameter dependencies of the recurrence times to which the bulk of the paper is devoted.

We first consider in Section 2 the case of recurrence in *uniform* quasi-periodic motion. As well known, in the presence of two incommensurate frequencies this motion reduces on a Poincaré surface of section to the twist map

$$x_{n+1} = F_\alpha(x_n) = x_n + \alpha \qquad \text{mod } 1 \tag{1}$$

where α is irrational. This mapping may also be seen as the simplest example of an interval exchange transformation, in which the two intervals $[0, 1-\alpha]$ and $]1-\alpha, 1]$ are exchanged under F_α. Ergodic properties of the corresponding interval exchange maps have been addressed by Kerckhoff[14] and Rauzy.[15] Section 2.1 is devoted to the derivation of the results of Lohöfer and Mayer mentioned above using an alternative, more physically-oriented method. In Sections 2.2 and 2.3 the dependence of the recurrence times on, respectively, the cell size and the intrinsic parameters is analysed by extensive numerical investigation and their high variability is brought out. The extension to high-dimensional tori is carried out in Section 2.4.

In Section 3 recurrence in non-uniform quasi-periodic motion is considered. The problem is first formulated in Section 3.1 for the two-parameter generalization of (1),

$$x_{n+1} = F_{\alpha, g}(x_n) = x_n + \alpha + g(x_n) \qquad \text{mod } 1 \tag{2}$$

where $g(x)$ is a nonlinear function of period 1. Using earlier results by Mayer[4] we show explicitly how the problem can be cast into a problem involving uniform, but phase space cell-depending dynamics for which the results of Section 2 may be applied. We subsequently illustrate in Section 3.2 the effects of non-uniformity in the behavior of recurrence times on the particular model of the sine circle map. The main conclusions are drawn in Section 4.

2. UNIFORM QUASI-PERIODIC MOTION

2.1. Two-Dimensional Uniform Quasi-Periodic Motion

Consider a torus T^2, that is, the phase space $[0, 2\pi] * [0, 2\pi]$. A two-dimensional uniform quasi-periodic motion on this torus is represented by two angular variables θ and ϕ whose evolution is parameterized by the time t:

$$\theta_t - \theta_0 = \omega_1 t \qquad \text{mod } 2\pi \tag{3}$$

$$\phi_t - \phi_0 = \omega_2 t \qquad \text{mod } 2\pi \tag{4}$$

where $\omega_1/\omega_2 \notin Q$ and consider, without loss of generality, $\omega_1 = |\omega_1|$ and $\omega_2 = |\omega_2|$. We are interested in determining the recurrence properties of such a dynamical system as a function of the specific partition chosen on the torus, the values of ω_1 and ω_2, and the size of the phase space cell. As this kind of uniform dynamics is also ergodic on the torus, the recurrence properties are uniform as well, implying that one may be limited to a single cell placed anywhere on the torus. Hereafter we choose, without loss of generality as will be shown below, a square cell C of side 2ε.

Hemmer *et al.*[2] derived an expression for the mean recurrence time $\langle T \rangle$ in the case of a linear chain of harmonically coupled masses. An early more general expression due to Smoluchowski[5] and applicable to any ergodic continuous time dynamical system is also available:

$$\langle T \rangle_\tau = \tau \frac{1 - P(C)}{P(C) - P(C, 0; C, \tau)} \tag{5}$$

where τ is the sampling period of the dynamics, $P(C)$ is the probability to be in cell C, and $P(C, 0; C, \tau)$ is the joint probability to be initially in cell C and to still be in it after a time τ. In the two-dimensional uniform case, the invariant density is $\rho(\theta, \phi) = 1/(2\pi)^2$ and

$$P(C) = (2\varepsilon/2\pi)^2 \tag{6}$$

$$P(C, 0; C, \tau) = \int_C d\theta'\, d\phi' \int_C d\theta\, d\phi\, \delta(\theta' - (\theta + \omega_1 \tau))\, \delta(\phi' - (\phi + \omega_2 \tau))\, \rho(\theta, \phi) \tag{7}$$

$$= \left(\frac{1}{2\pi}\right)^2 (2\varepsilon - \omega_1 \tau)(2\varepsilon - \omega_2 \tau) \qquad (2\varepsilon > \omega_1 \tau, \omega_2 \tau) \tag{8}$$

One thus gets from (5)–(7) in the continuous time limit $\tau \to 0$ and $\varepsilon \ll 1$

$$\langle T \rangle \simeq \frac{(2\pi)^2}{2\varepsilon(\omega_1 + \omega_2)} \tag{9}$$

In what follows we shall also be interested in more detailed properties of recurrence times, such as their variability around this mean value.

The general approach to the recurrence problem amounts to the search of pairs of positive integers k and l satisfying the following set of equations

$$\begin{aligned} \omega_1 t_p &= 2\pi k + \delta_1 \\ \omega_2 t_p &= 2\pi l + \delta_2 \end{aligned} \tag{10}$$

where t_p denotes the passage time of the trajectory in the cell and δ_1, δ_2 are real numbers in $[-\varepsilon, \varepsilon]$. Eliminating t_p, one is thus led to study the solutions of the following Diophantine inequality

$$|k - l\alpha| \leqslant \tilde{\varepsilon} \tag{11}$$

where $k, l \in N_0$, $\alpha = \omega_1/\omega_2 \notin Q$ and $\tilde{\varepsilon} = (\varepsilon/2\pi)(1 + (\omega_1/\omega_2))$. A recurrence time T is uniquely determined by a value Δk (Δl) separating two successive k (l) solutions of the Diophantine inequality, multiplied by the period associated to the frequency ω_1 (ω_2) plus a small correction associated to the finite size of the cell

$$T = \Delta k \frac{2\pi}{\omega_1} + O(\varepsilon) \tag{12}$$

$$= \Delta l \frac{2\pi}{\omega_2} + O(\varepsilon) \tag{13}$$

In the following, a particular recurrence time will be identified to the corresponding value Δk or Δl.

Now, finding the Δl's (and thus the Δk's too) from Eq. (11) is equivalent to solving the problem of the existence of gaps of an ordered set of integers in an exchange transformation formulated in the Introduction, the relevant interval being here

$$[0, \tilde{\varepsilon}] \cup [1 - \tilde{\varepsilon}, 1] \tag{14}$$

In the remaining of this Subsection we shall outline an alternative derivation of the results of Lohöfer and Mayer[12] on the existence of 2 or 3 discrete values of these gaps (recurrence times) which is more illustrative and suitable for the analysis of Subsections 2.2 to 2.4. As is well known, for given $\tilde{\varepsilon}$, relation (11) admits an infinity of solutions.[16] Let (k_n, l_n) be a particular pair of such solutions where the index n denotes the order (in time) in which they are realized. Recurrence of the trajectory in the cell after this nth passage is associated, then, with the pair of integers $(\Delta k_n, \Delta l_n)$ such that

$$\begin{aligned} \Delta k_n &= k_{n+1} - k_n \\ \Delta l_n &= l_{n+1} - l_n \end{aligned} \tag{15}$$

The main problem is thus to determine the full ordered set of ratios (for reasons that will be clear further) of different values of these integers, noted in the sequel by the superscript "$-$"

$$R = \left\{ \left(\frac{\Delta \bar{k}_j}{\Delta \bar{l}_j} \right) \right\} \qquad j = 1, 2(, 3) \tag{16}$$

According to (11), the differences

$$d_n = k_n - l_n \alpha \tag{17}$$

are bound by the inequality

$$-\tilde{\varepsilon} \leqslant d_n \leqslant \tilde{\varepsilon} \tag{18}$$

Setting

$$\bar{d}_1 = \Delta \bar{k}_1 - \Delta \bar{l}_1 \alpha \tag{19}$$

and noticing that Eq. (18) holds for $n+1$ as well as for n, one has (choosing n such that $k_{n+1} = k_n + \Delta \bar{k}_1$, $l_{n+1} = l_n + \Delta \bar{l}_1$)

$$-\tilde{\varepsilon} \leqslant d_n + \bar{d}_1 \leqslant \tilde{\varepsilon} \tag{20}$$

Since recurrence can occur anywhere in the cell, $\bar{d}_1$ can in principle take any value between $-2\tilde{\varepsilon}$ and $2\tilde{\varepsilon}$. Relation (20) imposes therefore two different types of constraints for d_n depending on the sign of $\bar{d}_1$:

$$-\tilde{\varepsilon} - \bar{d}_1 \leqslant d_n \leqslant \tilde{\varepsilon} \qquad \text{if} \quad \bar{d}_1 < 0 \tag{21}$$

$$-\tilde{\varepsilon} \leqslant d_n \leqslant \tilde{\varepsilon} - \bar{d}_1 \qquad \text{if} \quad \bar{d}_1 > 0 \tag{22}$$

In other words, depending on the sign of $\bar{d}_1$, d_n is bound to be in the set

$$S_{-}^{(1)} = (-\tilde{\varepsilon} - \bar{d}_1, \tilde{\varepsilon}) \tag{23}$$

or

$$S_{+}^{(1)} = (-\tilde{\varepsilon}, \tilde{\varepsilon} - \bar{d}_1) \tag{24}$$

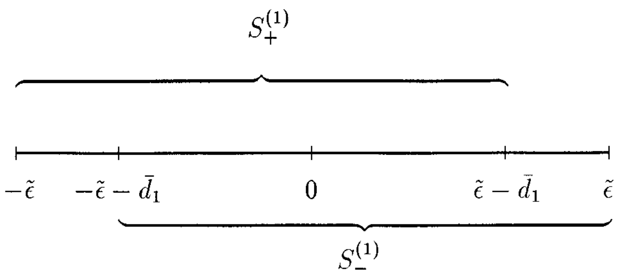

Fig. 1. A possible configuration for the sets $S_{\pm}^{(1)}$.

Figure 1 illustrates this for a particular choice of $\bar{d}_1$. The point is that sets $S_{\pm}^{(1)}$ are contained *within* the set $S = (-\tilde{\varepsilon}, \tilde{\varepsilon})$: $S_{\pm}^{(1)} \subset S$, $S_{\pm}^{(1)} \cap S \neq S$. As a result the phase space points belonging to the complement $S/S_{\pm}^{(1)}$ of $S_{\pm}^{(1)}$ within S cannot be connected by the recurrence time $(\Delta\bar{k}_1, \Delta\bar{l}_1)$. There has to be, therefore, a larger pair of integers $(\Delta\bar{k}_2, \Delta\bar{l}_2)$ determining recurrence in this latter set.

Let $\bar{d}_2 = \Delta\bar{k}_2 - \Delta\bar{l}_2\alpha$. Proceeding as before, we are led to define the sets

$$S_{-}^{(2)} = (-\tilde{\varepsilon} - \bar{d}_2, \tilde{\varepsilon}) \qquad (\bar{d}_2 < 0) \tag{25}$$

$$S_{+}^{(2)} = (-\tilde{\varepsilon}, \tilde{\varepsilon} - \bar{d}_2) \qquad (\bar{d}_2 > 0) \tag{26}$$

containing d_n, being understood that the latter is now supposed not to be in $S_{\pm}^{(1)}$, Eqs. (21)–(22). Figure 2 depicts two possible configurations of $S^{(2)}$ relative to $S^{(1)}$, corresponding to particular choices of signs and values of $\bar{d}_1$ and $\bar{d}_2$. In (a) $S_{+}^{(1)} \cup S_{-}^{(2)} = S$, meaning that recurrence occurs entirely through two discrete times. In (b) $(S_{+}^{(1)} \cup S_{-}^{(2)}) \cap S \neq S$. The phase space points in $S/(S_{+}^{(1)} \cup S_{-}^{(2)})$ recur therefore with a different, longer recurrence time associated with a new larger set of integers $(\Delta\bar{k}_3, \Delta\bar{l}_3)$. The process can be repeated until the sets $\{S_{\pm}^{(i)}\}$ cover fully the original set S.

A specification of the full set of distinct pairs $(\Delta\bar{k}_i, \Delta\bar{l}_i)$ determining entirely the recurrence properties can be achieved by using the continued fraction expansion of the real number α and the Farey tree. Indeed, we have seen (Eq. (19)) that the differences $\{\bar{d}_i\}$ involving the recurrence times $\{\Delta\bar{k}_i, \Delta\bar{l}_i\}$ satisfy the inequality $|\bar{d}_i| \leqslant 2\tilde{\varepsilon}$. Let us rewrite this result as

$$\left| \frac{\Delta\bar{k}_i}{\Delta\bar{l}_i} - \alpha \right| \leqslant \frac{2\tilde{\varepsilon}}{\Delta\bar{l}_i} \tag{27}$$

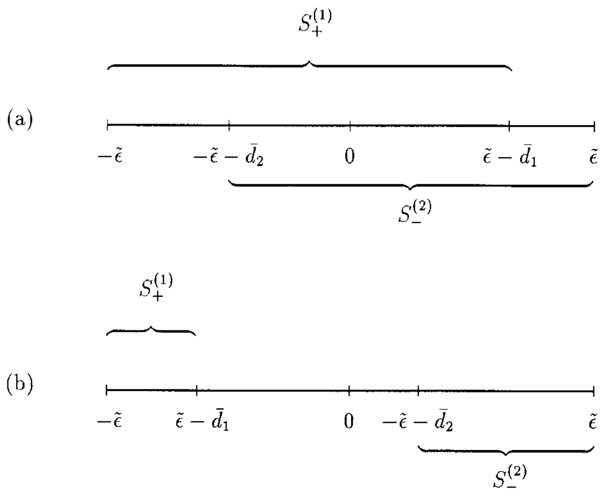

Fig. 2. Possible configurations for $S_+^{(1)}$ and $S_-^{(2)}$: (a) recurrence occurs entirely through two discrete times, (b) more than two times are involved in recurrence.

if $\alpha = \omega_1/\omega_2 < 1$, or

$$\left| \frac{\Delta \bar{l}_i}{\Delta \bar{k}_i} - \alpha \right| \leqslant \frac{2\tilde{\varepsilon}}{\Delta \bar{k}_i} \tag{28}$$

if α is defined as $\alpha = \omega_2/\omega_1 < 1$. This form is reminiscent of the classical problem of approximating an irrational α by rational numbers, written as ratios of two integers. Now, a rational number p/q, $p < q$, can be written as a finite regular continued fraction[16] $[a_1, a_2, a_3,..., a_n]$, whereas for an irrational number α, an infinite sequence $[a_1, a_2, a_3,..., a_n,...]$ is needed. Any such sequence truncated to a finite order produces a rational number which is referred to as an *approximant* to α. A well-known result of number theory is that these approximants are the *best* rational approximations to α, in the sense that any better rational approximation written as the ratio of two integers will display a larger denominator. Furthermore, the following properties are worth noting for later use: if $\tilde{p}_n/\tilde{q}_n$ and $\tilde{p}_{n-1}/\tilde{q}_{n-1}$ are, respectively, the nth and $(n-1)$th order approximant of α, then[16]

$$\frac{\tilde{p}_n}{\tilde{q}_n} - \frac{\tilde{p}_{n-1}}{\tilde{q}_{n-1}} = \frac{(-1)^{n-1}}{\tilde{q}_n \tilde{q}_{n-1}} \tag{29}$$

$$\left| \frac{\tilde{p}_n}{\tilde{q}_n} - \alpha \right| < \frac{1}{\tilde{q}_n \tilde{q}_{n+1}} < \frac{1}{a_{n+1} \tilde{q}_n^2} \leqslant \frac{1}{\tilde{q}_n^2} \xrightarrow[n \to \infty]{} 0 \tag{30}$$

The first relation implies, in particular, that while the absolute distances from α decrease monotonically as higher order approximants are taken, their signs are alternating. The following lemma[17] is also of great interest for further use:

Let α be a positive number, and let $\tilde{p}_n/\tilde{q}_n$ be the nth approximant ($n \geqslant 1$) of the regular continued fraction expansion of α in canonical form. Let p and q be positive integers such that $(p/q) \neq (\tilde{p}_n/\tilde{q}_n)$ with $0 < q \leqslant \tilde{q}_n$. Then

$$|p - q\alpha| \geqslant |\tilde{p}_{n-1} - \tilde{q}_{n-1}\alpha| > |\tilde{p}_n - \tilde{q}_n\alpha| \tag{31}$$

As well-known, the Farey tree[16] is a mathematical construction that permits a natural, exhaustive classification of the rationals in the interval $[0, 1]$. A "branch" of the Farey tree consists of a "mother to daughter" ordered sequence $\{p_n/q_n\}_1^\infty$, such that $p_n < p_{n+1}$, $q_n < q_{n+1}$ $\forall n > 0$. Each branch is unique and converges to an irrational number.

It may be seen that the successive approximants $\{\tilde{p}_n/\tilde{q}_n\}$ of α are those members of the Farey branch $\{p_n/q_n\}$ that are closest to α for each successive part of the branch at a positive or negative distance $(p_n/q_n) - \alpha$. In particular, their set forms a subset of $\{p_n/q_n\}$. Furthermore, by virtue of the lemma summarized in Eq. (31), all members p_n/q_n of the Farey branch situated between two successive approximants $(\tilde{p}_{j-1}/\tilde{q}_{j-1})$ and $(\tilde{p}_j/\tilde{q}_j)$ are at an absolute distance (in the sense of $|p_n - q_n\alpha|$) greater than the one of the lowest order approximant $(\tilde{p}_{j-1}/\tilde{q}_{j-1})$. Let us remark for further use that the coefficients a_j of the continued fraction expansion $\{a_j\}$ represent the number of non-approximant members, plus one, of the branch between the $(j-1)$th and the jth approximant. Those non-approximant members, which are sometimes called the "Nebenbrüche," may be expressed as linear combinations of two successive approximants, as follows:[9] if $\tilde{p}_k/\tilde{q}_k$ is the kth approximant of α, then the Nebenbrüche are

$$\frac{\tilde{p}_{k-1} + v\tilde{p}_k}{\tilde{q}_{k-1} + v\tilde{q}_k} \qquad (v = 1, 2,..., a_{k-1}) \tag{32}$$

The results summarized so far in this section are strong enough to identify the elements of the recurrence set R, Eq. (16), and to explain in a simple and quite geometrical way the behavior of the recurrence times as observed when the parameters ω_1, ω_2, and ε are varied.

The first point to be made is that the lemma, in conjunction with the fact that the approximants of the continued fraction are the best rational approximations to α, entails that $\Delta\bar{k}_1/\Delta\bar{l}_1$ must be the first member of

$\{\tilde{p}_n/\tilde{q}_n\}$ satisfying $|\bar{d}| \leqslant 2\tilde{\varepsilon}$. All other elements of R *must* belong to $\{p_n/q_n\}/(p_1/q_1,..., \Delta\bar{k}_1/\Delta\bar{l}_1)$ because even if they are not necessarily approximants and thus best rational approximations to α, they may have an absolute distance $|p_n - q_n\alpha|$ less than or equal to $2\tilde{\varepsilon}$ and there are no other fractions (not belonging to the branch) involved: the region of the tree delimited on the right side and on the left side by the members of the branch contains no fractions not belonging to the branch.

One wants now to show that for any set of values for the parameter set $\omega_1, \omega_2, \varepsilon$, the number of elements contained in R is only two or three (in which case the third element is the Farey-sum of the first two ones). Since $(\Delta\bar{k}_1/\Delta\bar{l}_1)$ is an approximant, say the ith one, $(\Delta\bar{k}_2/\Delta\bar{l}_2)$ will either be the $(i+1)$st approximant if $a_{i+1} = 1$, or, if $a_{i+1} > 1$, the first non-approximant (compatible with $|\bar{d}| \leqslant 2\tilde{\varepsilon}$) between $(\Delta\bar{k}_1/\Delta\bar{l}_1)$ and the $(i+1)$st approximant or the $(i+1)$st approximant itself. In either case, $\bar{d}_2$ has the opposite sign of $\bar{d}_1$. This implies that one could have, depending on $\bar{d}_1$ and $\bar{d}_2$,

$$S^1_- \cup S^2_+ = S \qquad \text{if} \quad \bar{d}_1 < 0 \tag{33}$$

or

$$S^1_+ \cup S^2_- = S \qquad \text{if} \quad \bar{d}_1 > 0 \tag{34}$$

This will occur whenever $|\bar{d}_1 - \bar{d}_2| \leqslant 2\tilde{\varepsilon}$. R contains then only two elements: $R = \{(\Delta\bar{k}_1/\Delta\bar{l}_1), (\Delta\bar{k}_2/\Delta\bar{l}_2)\}$. If this happens not to be the case then one has to consider a third recurrence time fraction, whose numerator and denominator are, respectively, larger than $\Delta\bar{k}_2$ and $\Delta\bar{l}_2$. The smallest possible such fraction is the next fraction on the branch after $\Delta\bar{k}_2/\Delta\bar{l}_2$, which is necessarily the Farey-sum of $\Delta\bar{k}_1/\Delta\bar{l}_1$, and $\Delta\bar{k}_2/\Delta\bar{l}_2$. This follows from the fact that all members of the branch are the result of the Farey summation of the previous member of the branch and the approximant immediately preceding this member, which is automatically the case for $(\Delta\bar{k}_3/\Delta\bar{l}_3)$. One has therefore

$$\frac{\Delta\bar{k}_3}{\Delta\bar{l}_3} = \frac{\Delta\bar{k}_1 + \Delta\bar{k}_2}{\Delta\bar{l}_1 + \Delta\bar{l}_2} \tag{35}$$

and

$$\bar{d}_3 = \bar{d}_1 + \bar{d}_2 \tag{36}$$

which, knowing that $\bar{d}_1$ and $\bar{d}_2$ have opposite signs, automatically implies that $|\bar{d}_3| \leqslant 2\tilde{\varepsilon}$. Defining

$$S^{(3)} = (-\tilde{\varepsilon} - (\bar{d}_1 + \bar{d}_2), \tilde{\varepsilon}) \qquad \text{if} \quad (\bar{d}_1 + \bar{d}_2) < 0 \tag{37}$$

$$S^{(3)} = (-\tilde{\varepsilon}, \tilde{\varepsilon} - (\bar{d}_1 + \bar{d}_2)) \qquad \text{if} \quad (\bar{d}_1 + \bar{d}_2) > 0 \tag{38}$$

one finds

$$S^{(1)}_{\mp} \cup S^{(2)}_{\pm} \cup S^{(3)} = S \tag{39}$$

implying that R contains three and only three elements, $R = \{(\Delta\bar{k}_1/\Delta\bar{l}_1), (\Delta\bar{k}_2/\Delta\bar{l}_2), ((\Delta\bar{k}_1 + \Delta\bar{k}_2/(\Delta\bar{l}_1 + \Delta\bar{l}_2))\}$. Note that these recurrence times are then necessarily relatively prime, as they all belong to the same Farey branch. We have thus proved quite directly that at least two recurrence times appear and that three recurrence times are enough for a uniform dynamics on a T^2 torus.

We turn now to numerical investigations of the solutions of inequality (11). We find the mean recurrence time to be in excellent agreement with expression (9). The specific values of the discrete recurrence times are found to be strongly dependent on the precise set of parameter values and undergo abrupt transitions toward increasing values when $\varepsilon \to 0$. Figure 3 illustrates this phenomenon for a particular value of α. It is clearly seen that while the first (the smallest) recurrence time remains constant, the second and third recurrence times can only increase by the value of the first

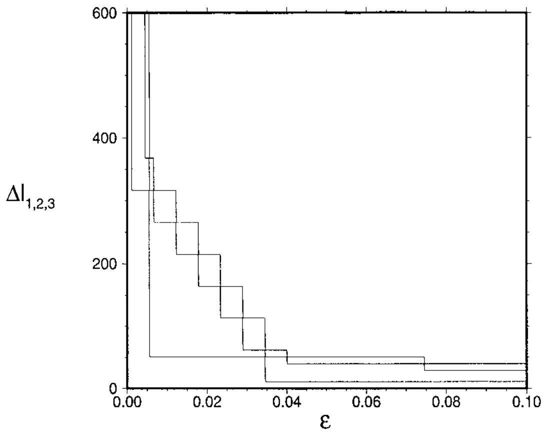

Fig. 3. Values of Δl separating two successive solutions of Eq. (11) as a function of the cell half-size ε. Parameter values $\omega_1 = 1$, $\omega_2 = 1.378264538947351816\ldots$, and cell size resolution $\Delta\varepsilon = 10^{-5}$.

recurrence time, and that when this one changes it takes the value of the second one just before the transition, while the second one takes the value of the third one just before the transition.

The following subsections will provide the necessary tools to understand in detail, and reproduce, the rich behavior observed.

2.2. Cell Size Dependence of Recurrence Times

Suppose that one has fixed one frequency set ω_1, ω_2 and some cell size and knows the resulting $(\Delta\bar{k}_1/\Delta\bar{l}_1)$, $(\Delta\bar{k}_2/\Delta\bar{l}_2)$, $(\Delta\bar{k}_3/\Delta\bar{l}_3)$. In this section we show how, on this basis, one may determine $\langle T \rangle$, its higher moments, the succession of the two or three recurrence times (that is, their order of appearance) thereby generating all the solutions of Eq. (11) for all cell sizes smaller than the original one. We introduce for this purpose the "distance cone," a construct which permits us to determine what the recurrence times are and how they vary with ε.

The distance cone is defined as the part of the half-plane $(\varepsilon, \bar{d})$ delimited by the lines $\bar{d}=2\tilde{\varepsilon}$ and $\bar{d}=-2\tilde{\varepsilon}$, as illustrated in Fig. 4. Plotting the horizontal lines $\bar{d}=\bar{d}_1$, $\bar{d}=\bar{d}_2$, and $\bar{d}=\bar{d}_3$ inside the cone, one can then determine how the recurrence times will evolve as $\varepsilon \to 0$. To see this, let us start from some ε_0 (in the concrete case considered in the figure, $\varepsilon_0 = 0.1$). As ε decreases, one of the lines $\bar{d}=\bar{d}_1$ or $\bar{d}=\bar{d}_2$ (e.g., the one corresponding to the second recurrence time, marked as 2 in the figure) will leave the cone. This corresponds precisely to the value of ε for which $|\bar{d}_1| = 2\tilde{\varepsilon}$ (or $|\bar{d}_2| = 2\tilde{\varepsilon}$, as is the case in the figure). The associated recurrence time will

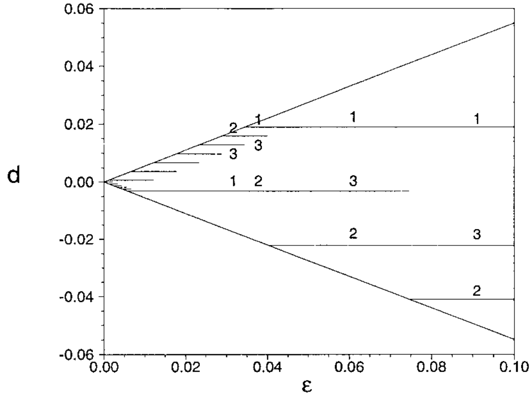

Fig. 4. Distance cone for $\alpha = 1/1.378264538947351816\ldots$. The numbers 1, 2, 3 are associated to the distances $\bar{d}_1, \bar{d}_2, \bar{d}_3$ related to the first, second, and third recurrence times.

then disappear, allowing for only two recurrence times at the transition (the two remaining ones). These become the first and second recurrence time, and because one always has $\bar{d}_3 = \bar{d}_1 + \bar{d}_2$, it is clear that $|\bar{d}_1 - \bar{d}_2| = 2\tilde{\varepsilon}$ with the new first and second recurrence times at the transition point. This means that past this transition point, as ε keeps decreasing, one finds $|\bar{d}_1 - \bar{d}_2| > 2\tilde{\varepsilon}$, implying the immediate appearance of a third recurrence time. Generically one therefore has three recurrence times on the parameter space ε, whatever $\alpha \notin Q$ is.

Proceeding in this way, one may determine entirely what the recurrence times are and how they vary for all $\varepsilon \leqslant \varepsilon_0$: whenever a horizontal line leaves the cone a new one appears whose ordinate is the sum of ordinates of the two remaining lines, the associated recurrence time being the sum of the two remaining ones.

We now derive the explicit dependence of recurrence times moments on the elements of the set R. Since $d_n \notin Q\ \forall n > 0$ and $d_n \neq d_m\ \forall m, n > 0$ $(m \neq n)$, setting

$$D = \{d_n\}_1^\infty \tag{40}$$

one has

$$D = [-\tilde{\varepsilon}, \tilde{\varepsilon}]/Q \tag{41}$$

Using the uniformity of the distribution of $\{d_n\}_1^\infty$ on $[-\tilde{\varepsilon}, \tilde{\varepsilon}]/Q$ and the results on the distance cone one may calculate the mean recurrence time and its higher moments for all $\varepsilon \leqslant \varepsilon_0$. To this end, we introduce

$$\begin{aligned} D_1 &= S_{\pm}^{(1)} \\ D_2 &= S_{\mp}^{(2)}/S_{\pm}^{(1)} \\ D_3 &= S^{(3)}/(S_{\pm}^{(1)} \cup S_{\mp}^{(2)}) \end{aligned} \tag{42}$$

and

$$\begin{aligned} f_1 &= \mu(D_1)/2\tilde{\varepsilon} \\ f_2 &= \mu(D_2)/2\tilde{\varepsilon} \\ f_3 &= \mu(D_3)/2\tilde{\varepsilon} \end{aligned} \tag{43}$$

where $\mu(D_i)$ is the invariant measure of D_i. Neglecting finite size effects, one has then for $\langle T \rangle$ and its standard deviation σ

$$\langle T \rangle = (f_1\, \Delta\bar{k}_1 + f_2\, \Delta\bar{k}_2 + f_3\, \Delta\bar{k}_3)\, \frac{2\pi}{\omega_1} \tag{44}$$

$$\sigma = \sqrt{\left(\frac{2\pi}{\omega_1}\right)^2 (f_1\, \Delta\bar{k}_1{}^2 + f_2\, \Delta\bar{k}_2{}^2 + f_3\, \Delta\bar{k}_3{}^2) - \langle T \rangle^2} \tag{45}$$

Higher moments can be expressed in a similar way. These expressions are found to be in excellent agreement with the results of numerical experiments. Note that in the present study we chose square cells of side 2ε for mathematical convenience. Our analysis shows that what really matters is the cross-section of the cell through the flow on the torus: the shape itself is not important, as long as the size remains small.

Actually, one can cast the original dynamics in a form that allows for a full deterministic description of the succession of the recurrence times, which is of central importance in terms of prediction skills. Indeed, one may express the general solution of Eq. (11) as:

$$\begin{aligned} k(n) &= n_1(n)\, \Delta\bar{k}_1 + n_2(n)\, \Delta\bar{k}_2 \\ l(n) &= n_1(n)\, \Delta\bar{l}_1 + n_2(n)\, \Delta\bar{l}_2 \end{aligned} \tag{46}$$

The positive integers $n_1(n), n_2(n)$ are determined in terms of the solutions of the following piecewise linear map:

$$x_{n+1} = f(x_n) = \begin{cases} x_n + \bar{d}_1 & \text{if} \quad x_n \in D_1 \\ x_n + \bar{d}_2 & \text{if} \quad x_n \in D_2 \\ x_n + \bar{d}_3 & \text{if} \quad x_n \in D_3 \end{cases} \tag{47}$$

where $x_n \in [-\tilde{\varepsilon}, \tilde{\varepsilon}]$ and the initial condition x_0 equals the distance $\bar{d}_i = \Delta\bar{k}_i - \Delta\bar{l}_i \alpha$ associated to the smallest recurrence time $(\Delta\bar{k}_i, \Delta\bar{l}_i)$ satisfying $|\bar{d}| \leqslant \tilde{\varepsilon}$ (this condition may be checked to be automatically fulfilled for at least one recurrence time, as it obviously should). Specifically,

$$\begin{pmatrix} n_1(n) \\ n_2(n) \end{pmatrix} = \begin{pmatrix} n_1(1) \\ n_2(1) \end{pmatrix} + \sum_{j=2}^{n} \begin{pmatrix} \xi_j \\ \eta_j \end{pmatrix} \tag{48}$$

where

$$\begin{pmatrix} n_1(1) \\ n_2(1) \end{pmatrix} = \begin{pmatrix} 1 \\ 0 \end{pmatrix} \qquad \text{if} \quad |\bar{d}_1| \leqslant \tilde{\varepsilon} \tag{49}$$

$$\begin{pmatrix} n_1(1) \\ n_2(1) \end{pmatrix} = \begin{pmatrix} 0 \\ 1 \end{pmatrix} \qquad \text{if} \quad |\bar{d}_1| > \tilde{\varepsilon}, \quad |\bar{d}_2| \leqslant \tilde{\varepsilon} \tag{50}$$

$$\begin{pmatrix} n_1(1) \\ n_2(1) \end{pmatrix} = \begin{pmatrix} 1 \\ 1 \end{pmatrix} \qquad \text{if} \quad |\bar{d}_1| > \tilde{\varepsilon}, \quad |\bar{d}_2| > \tilde{\varepsilon} \tag{51}$$

and

$$\begin{pmatrix} \xi_j \\ \eta_j \end{pmatrix} = \begin{pmatrix} 1 \\ 0 \end{pmatrix} \qquad \text{if} \quad x_j \in D_1 \tag{52}$$

$$\begin{pmatrix} \xi_j \\ \eta_j \end{pmatrix} = \begin{pmatrix} 0 \\ 1 \end{pmatrix} \qquad \text{if} \quad x_j \in D_2 \tag{53}$$

$$\begin{pmatrix} \xi_j \\ \eta_j \end{pmatrix} = \begin{pmatrix} 1 \\ 1 \end{pmatrix} \qquad \text{if} \quad x_j \in D_3 \tag{54}$$

This procedure amounts, therefore, to casting recurrence in the form of a symbolic dynamics involving the three "states" D_1, D_2 and D_3. It is automatically checked that this map is also an interval exchange transformation, and is simply map (1) restricted to the interval $[0, \tilde{\varepsilon}] \cup [1-\tilde{\varepsilon}, 1]$, showing the ergodic properties discussed in ref. 14 and references therein.

The following observations also follow from the properties of the map of Eq. (47). First, the temporal sequence of the 2 or 3 different recurrence times is itself quasi-periodic. Indeed, as this map has a uniform invariant density and slopes everywhere equal to one, no periodic or chaotic motion can occur. Its dynamics must thus be quasi-periodic, implying a similar property for its symbolic dynamics as well. Second, there will always be some forbidden transitions in the temporal succession of the recurrence times, whatever the number of recurrence times is. An explicit $2 * 2$ or $3 * 3$ transition probability matrix $\mathbf{W}$ between the different recurrence times may be constructed, given the values of the D_1, D_2(, D_3) state boundaries. The elements of this matrix are given by the following expression:

$$W_{ij} = \frac{\mu(f(D_i) \cap D_j)}{\mu(D_i)} \tag{55}$$

where $\mu(D_i)$ is the measure of the state D_i and f is given by (47), with the property

$$\sum_{j=1}^{2(3)} W_{ij} = 1 \qquad \forall i = 1, 2(, 3) \tag{56}$$

At the specific values of ε where only 2 recurrence times are allowed (when $|\bar{d}_1 - \bar{d}_2| = 2\tilde{\varepsilon}$), it is clear that if $|\bar{d}_{1(2)}| \geqslant \tilde{\varepsilon}$ then $W_{11} = 0$ ($W_{22} = 0$), implying that the transitions $\Delta\bar{k}_1 \leftrightarrow \Delta\bar{k}_1$ ($\Delta\bar{k}_2 \leftrightarrow \Delta\bar{k}_2$) are forbidden. Analoguous expressions for the determination of forbidden transitions may be derived when 3 recurrence times are present. As an example, for the parameter set ($\alpha = 1/\sqrt{13}, \varepsilon = 0.0096$), for which one has three recurrence times, $\mathbf{W}$ has the form

$$\mathbf{W} = \begin{pmatrix} 0 & 1 & 0 \\ 0.38045 & 0.28666 & 0.33288 \\ 0 & 1 & 0 \end{pmatrix} \tag{57}$$

showing that the transitions $\Delta\bar{k}_1 \leftrightarrow \Delta\bar{k}_1$, $\Delta\bar{k}_1 \leftrightarrow \Delta\bar{k}_3$, and $\Delta\bar{k}_3 \leftrightarrow \Delta\bar{k}_3$ are in this case forbidden.

The construction of higher-order matrices $(W_{i,\, j,\dots,\, n})$, $i, j,\dots, n \leqslant 3$ whose elements represent the probability of observing a sequence $\Delta\bar{k}_i$, $\Delta\bar{k}_j,\dots, \Delta\bar{k}_n$ of recurrence times is of a more complicated nature as it implies the study of multiple projection of (sub-)intervals of D_1, D_2 and D_3 under map (47). The knowledge of such probabilities is essential though in the understanding of the structure of the correlation function of the observed recurrence times sequence. Such correlations are strongly dependent on the respective sizes of D_1, D_2, D_3 and thus on α and ε.

2.3. Branch Structure Dependence of Recurrence Times

The direct computation of the recurrence times $\Delta\bar{k}$ ($\Delta\bar{l}$) from Eq. (11) for all values of $\varepsilon \to 0$ reveals that the set of all observed $\Delta\bar{k}/\Delta\bar{l}$ fills in (completely), as it should, the set $\{p_n/q_n\}$ of the Farey branch converging to α, that is, all $\Delta\bar{k}/\Delta\bar{l}$ belong to $\{p_n/q_n\}$. The particular fractions of recurrence times for a given set of parameter values need not be neighbors in the set $\{p_n/q_n\}$, as this depends on the structure of the branch.

The specific structure of the branch may be quantified by the complexity of the corresponding sequence $\{a_j\}$: since the elements a_j represent the number, plus one, of non approximant members of the branch between the jth and $(j-1)$th approximant, a "complex" sequence of numbers means a complex branch structure (the branch winds in a complex way), and a regular, "simple" sequence means a simple branch structure, as for example for $\alpha = \sqrt{5} - 1/2$ and $\alpha = 1/\sqrt{2}$ for which the continued fraction expansions are, respectively, $[1, 1, 1,\dots, 1,\dots]$ and $[1, 2, 2,\dots, 2,\dots]$ (periodic structures). We therefore expect that the structure of the branch should have profound consequences on the underlying phenomenon of recurrence and, in particular, on the behavior of the standard deviation σ of the recurrence times since a complex branch structure may be responsible for a considerable dispersion of recurrence times. For instance, if $\Delta\bar{k}_1/\Delta\bar{l}_1$ is the jth approximant, then $\Delta\bar{k}_2/\Delta\bar{l}_2$ may be up to the $(j+1)$th approximant, in which case the number of elements between $\Delta\bar{k}_1/\Delta\bar{l}_1$ and $\Delta\bar{k}_2/\Delta\bar{l}_2$ is $a_{j+1}-1$. Depending on where $\Delta\bar{k}_1/\Delta\bar{l}_1$ is on the branch (that is, on the value of ε), a_{j+1} may be a large number, implying $\Delta\bar{k}_1 \ll \Delta\bar{k}_2$, which in turn may entail a great standard deviation of recurrence times, assuming that one has $\mu(D_1) \simeq \mu(D_2)$.

In this respect one sees from relation (30), that irrationals having a regular continued fraction expansion $\{a_j\}$ where a_j are large integers have the property to be particularly well approximated by their approximants, that is the convergence toward α is fast, while an expansion with small integers entails a slow convergence. This means in turn that irrationals that are not well approximated by rationals (called Diophantine numbers) are expected, given any ε, to generate a lower standard deviation than irrationals well approximated by rationals. As an explicit illustration, consider the least well approximated number, the (reciprocal of) Golden Mean: $\alpha = (\sqrt{5}-1)/2$. Its branch structure being very simple (all members of the branch are approximants), one has that for all fixed value of ε the recurrence times fractions are neighbors on the branch and thus generate a low standard deviation.

We next investigate the dependence of the recurrence times and the relative standard deviation on α at fixed value of ε. Figure 5 depicts the result concerning the recurrence times. In order to understand the origin of the structures appearing on the figure, let us consider a certain fraction p_1/q_1 and inquire, for what values of α will this be the first recurrence time fraction. Clearly, for any given ε, p_1/q_1 will be the first recurrence time for all $\alpha \in [((p_1-2\tilde{\varepsilon})/q_1), ((p_1+2\tilde{\varepsilon})/q_1)]$ if there are no other lower-level fractions p_n^*/q_n^* (that is, p_n^* and q_n^* are smaller integers than p_1 and q_1) such that

$$\left[\frac{p_n^*-2\tilde{\varepsilon}}{q_n^*}, \frac{p_n^*+2\tilde{\varepsilon}}{q_n^*}\right] \cap \left[\frac{p_1-2\tilde{\varepsilon}}{q_1}, \frac{p_1+2\tilde{\varepsilon}}{q_1}\right] \neq \varnothing \tag{58}$$

Otherwise, p_1/q_1 would be the first recurrence time fraction for all α ($\in\Re$!) such that

$$\alpha \in \left[\frac{p_1-2\tilde{\varepsilon}}{q_1}, \frac{p_1+2\tilde{\varepsilon}}{q_1}\right] \Big/ \left(\bigcup_n \left[\frac{p_n^*-2\tilde{\varepsilon}}{q_n^*}, \frac{p_n^*+2\tilde{\varepsilon}}{q_n^*}\right]\right) \tag{59}$$

The figure shows that the lower the level of p_1/q_1 the greater the range of α values around p_1/q_1 that will satisfy

$$\left|\frac{p_1}{q_1} - \alpha\right| \leqslant \frac{2\tilde{\varepsilon}}{q_1} \tag{60}$$

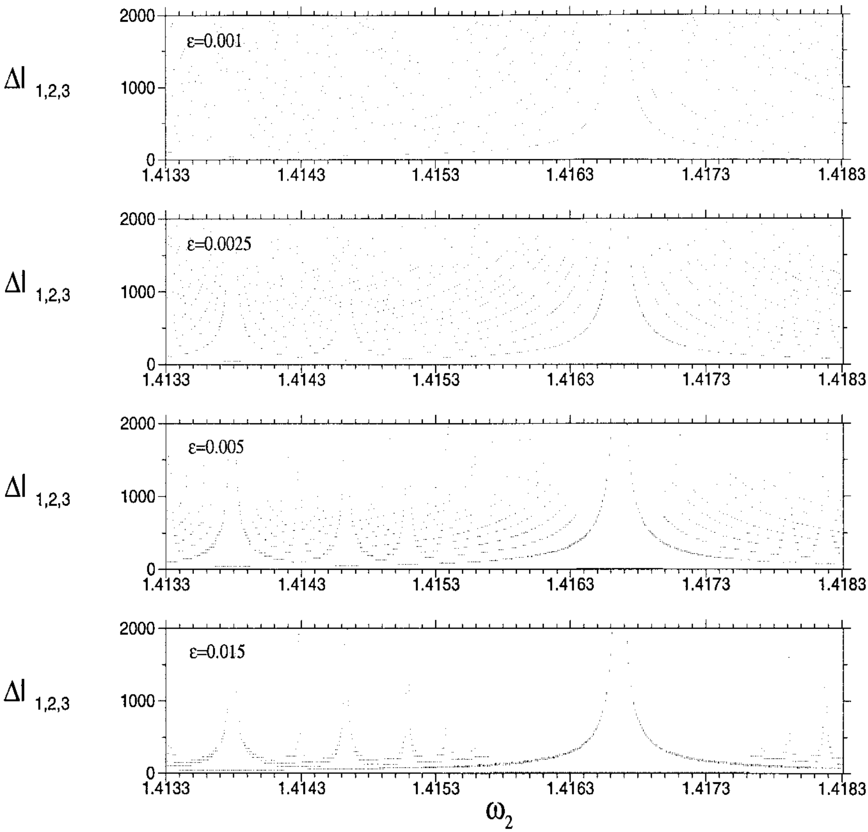

Fig. 5. Typical dependence of the two or three recurrence times ($\Delta\bar{l}_{1,2,3}$) on α, for different values of ε ($\omega_1 = 1$, $\Delta\omega_2 = 10^{-6}$).

Furthermore, lowering the value of ε decreases the range. This may be understood through the following observation: p_1/q_1 being an approximant, one has (cf. Eq. (30))

$$\left|\frac{p_1}{q_1} - \alpha\right| < \frac{1}{q_1 q_2} \tag{61}$$

where p_2/q_2 is the next approximant after p_1/q_1. This means that q_2 may increase substantially as $\alpha \to (p_1/q_1)$, and this increase will be more pronounced if q_1 is small. One thus finds that the lower the level of p_1/q_1, the higher the level of p_2/q_2 (and p_3/q_3) as $\alpha \to (p_1/q_1)$ and the greater the range of α-values where p_1/q_1 is the first recurrence time fraction. This phenomenon generates the great number of "trumpet-like" structures of varying height observed on Fig. 5.

The above spreading of the recurrence times is naturally reflected by the behavior of their (relative) standard deviation, as illustrated on Fig. 6. Here, the trumpet-like structures are more evident. They become denser with decreasing value of ε since in this case the range of α-values for the first recurrence time decreases, giving rise to wide dispersion of first recurrence times. The point to be stressed is that a slight variation of cell size and/or frequency may dramatically change the recurrence times themselves and thus the fluctuations around the mean recurrence time.

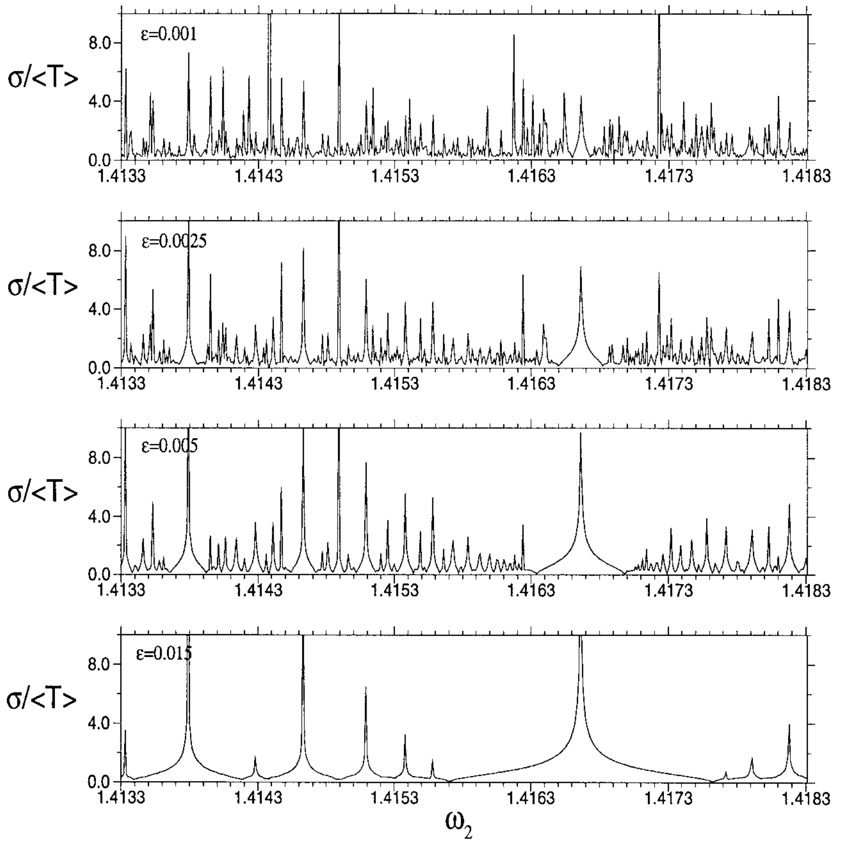

Fig. 6. Dependence of the relative standard deviation on α, for different values of ε and the parameter values of Fig. 5.

2.4. Generalization to n-Dimensional Tori

In this Section we comment on the extension of the above results to uniform quasi-periodic motion involving n $(n>2)$ irrationally related frequencies ω_i, $i=1,\ldots,n$. Choosing a phase space cell in the form of a hypercube of side 2ε, one can extend straightforwardly Eq. (5). For instance, for $n=3$, one thus obtains for small ε the explicit form

$$\langle T\rangle \simeq \frac{(2\pi)^3}{(2\varepsilon)^2\,(\omega_1+\omega_2+\omega_3)} \tag{62}$$

As before, the numerical simulation is in excellent agreement with the above value and reveals, furthermore, the existence of a limited number of distinct recurrence times. Unfortunately, the higher dimensionality seems to bring out new features that do not allow us to analyze the problem in full detail.

Let us illustrate this in the case $n=3$. Performing the same algebra that led to Eq. (11), now with three frequencies $\omega_1, \omega_2, \omega_3$, the Diophantine inequalities to be solved are

$$|k-l\alpha_1| \leqslant \tilde{\varepsilon}_1 \tag{63}$$

$$|k-m\alpha_2| \leqslant \tilde{\varepsilon}_2 \tag{64}$$

$$|l-m\alpha_3| \leqslant \tilde{\varepsilon}_3 \tag{65}$$

where $k, l, m \in N_0$, $\alpha_1=\omega_1/\omega_2$, $\alpha_2=\omega_1/\omega_3$, $\alpha_3=\omega_2/\omega_3$ such that $0<\alpha_i<1$, and $\tilde{\varepsilon}_i=(\varepsilon/2\pi)(1+\alpha_i)$. This new set of inequalities may be interpreted as a two-dimensional *simultaneous* "super"-approximation problem for the integer k, that is, a two-dimensional simultaneous approximation problem[18] for k (Eqs. (63) and (64)) with an additional constraint imposed on l and m (Eq. (65)). A similar problem will arise for all $n>2$ where (63)–(65) will be replaced by $n(n-1)/2$ equations.

The set of inequalities (63)–(65) may be reduced, considering each inequality separately and their associated symbolic dynamics, to a set of Diophantine expressions, each one similar to (46). One is thus led to solve a set of three Diophantine expressions whose coefficients are given by three different symbolic dynamics. It therefore seems impossible to extract in a straightforward way as enlightening results as in a two-dimensional case. The number of distinct recurrence times observed depends on α_i and ε, and is usually around 8 or 9 (and up to 15 or more). On the other hand, the constraints imposed on k (l, m) by Eqs. (63)–(65) are too strong to allow for all the recurrence times fractions $\Delta\bar{k}_i/\Delta\bar{l}_i$ $((\Delta\bar{k}_i/\Delta\bar{m}_i), (\Delta\bar{l}_i/\Delta\bar{m}_i))$ to be exclusively part of the Farey branch converging to α_1 (α_2, α_3): the specific values of $\Delta\bar{k}_i/\Delta\bar{l}_i$ are linear Farey-combinations of the $\Delta\bar{k}'_1/\Delta\bar{l}'_1$ and $\Delta\bar{k}'_2/\Delta\bar{l}'_2$ that would be observed if Eqs. (63)–(65) were solved independently, those combinations being thus in general such that they do not belong to the branch converging to α_1. Figure 7 illustrates the evolution of the recurrence times and their relative standard deviation with ε for $\omega_1=1$, $\omega_2=\sqrt{2}$, $\omega_3=\sqrt{3}$. Figures 8 and 9 illustrate the behavior of these quantities as $\omega_1, \omega_2, \varepsilon$ are kept fixed and ω_3 is varied. The evolution of the recurrence times presents embedded trumpet-like structures of a more complex nature than in the two-dimensional case, reflecting the new features brought by the higher dimensionality. Yet, despite this complex embedding of trumpet-like structures, the evolution of the relative standard deviation is quite similar to the two-dimensional case, see Fig. 6.

In short, high-dimensional uniform quasi-periodic motion also displays great sensitivity to variations of parameters as far as fluctuations around the mean recurrence time are concerned.

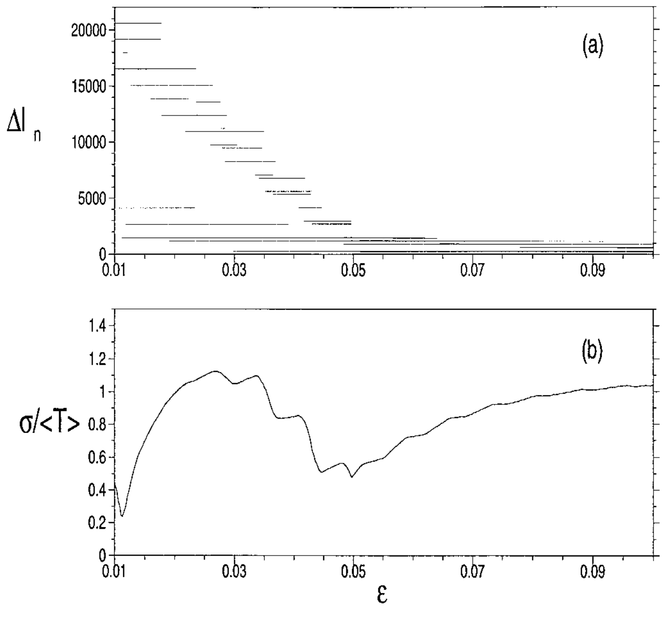

Fig. 7. Recurrence times (a) and relative standard deviation (b) as ε varies, as obtained from the first 10000 solutions of Eqs. (63)–(65) ($\omega_1=1$, $\omega_2=2^{1/2}$, $\omega_3=3^{1/2}$, $\Delta\varepsilon=10^{-4}$).

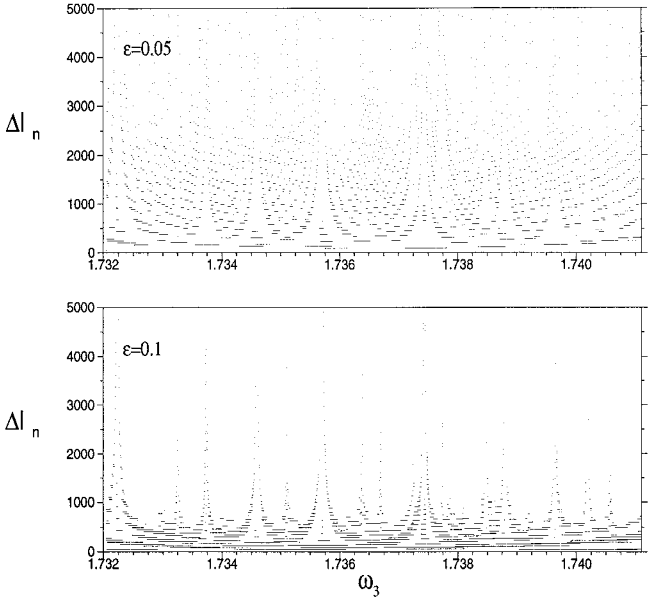

Fig. 8. Typical dependence of the recurrence times ($\Delta \bar{l}_n, n = 1,...$) on $\alpha_{1,2,3}$, for different values of ε as ω_3 varies ($\omega_1 = 1$, $\omega_2 = 2^{1/2}$, $\Delta\omega_3 = 10^{-5}$).

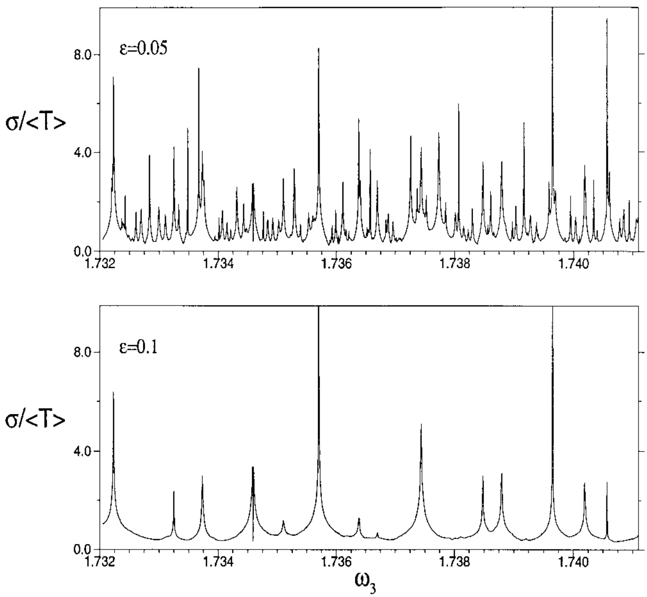

Fig. 9. Dependence of the relative standard deviation on ω_3 for different values of ε and parameter values of Fig. 8.

3. NON-UNIFORM QUASI-PERIODIC MOTION

It is well known that nonlinearities generally induce non-uniformities in the spreading of the trajectories and in the invariant density of a dynamical system in the underlying phase space. As a consequence, mean recurrence times may be expected to be depending on the position of the corresponding phase-space cell. One may also expect different discrete recurrence times and different fluctuations around local mean recurrence times. In this Section we outline the main steps toward the extension of the recurrence times properties of uniform quasi-periodic motion to non-uniform quasi-periodic motion. We will limit ourselves to the two-dimensional case as it will be clear further that the generalization to higher-dimensional tori goes along the same lines as in the uniform case. The persistence of two or three recurrence times in two-dimensional non-uniform quasi-periodic motion was anticipated by Mayer.[4]

3.1. General Formulation

As mentioned in the Introduction, non-uniform quasi-periodic motion reduces on a Poincaré surface of section to a nonlinear twist map $f(x_n)$, of the form of Eq. (2). Let us suppose f: $T^1 \to T^1$ be an orientation preserving circle homeomorphism, that is, f is continuous with continuous inverse and preserves the order of points on the circle T^1. We define the *rotation number*, or *winding number*, of f as

$$\rho = \lim_{n \to \infty} \frac{x_n - x_0}{n} \tag{66}$$

with x_n computed without a mod 1 constraint in f, that is, from a *lift* of f.

When limit (66) exists, it measures the average rotation per iterate of f. It is independent of x_0 and gives valuable information concerning the kind of dynamics: if ρ is rational, say $\rho = p/q$ where p and q are relatively prime integers, then the motion on the two-torus is periodic-phase locked (with period q), and if ρ is irrational then the motion is quasi-periodic. The inverse is also true.

Suppose now f, g: $T^1 \to T^1$ are orientation preserving circle homeomorphisms. f and g are called *conjugate* if there exists a homeomorphism h: $T^1 \to T^1$ such that $h \circ f = g \circ h$. The following results can then be established (for a review see, e.g., Walsh[19]):

— If f: $T^1 \to T^1$ is a C^1-diffeomorphism with $\rho = \alpha \notin Q$, and if f' has bounded variation, then f is conjugate to the rigid rotation r_α: $x \to x + \alpha$

mod 1 (Denjoy's Theorem). The rotation number ρ is invariant under a continuous change of variables.

— If $f, g: T^1 \to T^1$ are conjugate orientation preserving homeomorphism, then they have the same rotation number.

Consider next N equally sized non-overlapping cells in $[0, 1]$. The recurrence of the phase-space trajectory into a given phase-space cell may be expressed by the following inequality:

$$|k-(x_n-x_0)| \leqslant \varepsilon \tag{67}$$

or

$$(x_n-x_0) \bmod 1 \in [0, \varepsilon] \cup [1-\varepsilon, 1] \tag{68}$$

where $\varepsilon = 1/2N$, x_0 is the center point of the chosen cell, x_n is the nth image of x_0 by the lift of map f, and k is an integer.

The values of n for which Eqs. (67) or (68) are satisfied are the passage times of the phase-space trajectory into the cell centered around x_0 on the Poincaré section, normalized by the time between two successive crossings. The discrete recurrence times in that cell are then the differences between successive values of n, solutions of Eqs. (67) or (68).

Now, the existence of a conjugacy $h(x)$ to a pure irrational rotation

$$x_{n+1} = x_n + \rho \qquad \bmod 1 \tag{69}$$

guarantees that there exists a continuous change of variable $u(x)$ that brings the non-uniform invariant density $\rho_s^{nu}(x)$ of f to a uniform invariant density $\rho_s^u(x)$. Writing

$$\rho_s^{nu}(x) = \rho_s^{nu}(u(x)) \frac{du}{dx} \tag{70}$$

$$= \rho_s^u(x) \frac{du}{dx} \tag{71}$$

where $\rho_s^u(x) = 1 \;\; \forall x$, one finds

$$u(x) = \int_0^x \rho_s^{nu}(y)\, dy \tag{72}$$

On the other hand, the conjugacy will deform the cells of the partition differently, depending on their position. To account for this we rewrite Eq. (67) in the form

$$|k-(x_n-x_0)| \leqslant \frac{\Delta x}{2} = \frac{(x_0+\varepsilon)-(x_0-\varepsilon)}{2} \tag{73}$$

Under the conjugacy h,

$$x_n - x_0 \to n\rho \tag{74}$$

and

$$\frac{(x_0+\varepsilon)-(x_0-\varepsilon)}{2} \to \frac{1}{2}\int_{x_0-\varepsilon}^{x_0+\varepsilon} \rho_s^{nu}(y)\,dy = \frac{\mu(C)}{2} \tag{75}$$

where $\mu(C)$ is the invariant measure of the cell C around x_0. Equation (67) therefore becomes

$$|k-n\rho| \leqslant \frac{\mu(C)}{2} \tag{76}$$

and we showed in the first part of this paper how the recurrence times behavior is determined by the properties of convergence of the continued fraction representation of the irrational ρ.

The conjugacy allows us then to reduce the original problem involving non-uniform dynamics to a problem involving uniform, but phase-space cell depending, dynamics for which the previous results may be applied.

It is interesting to note that what really matters in this respect is the invariant measure of the cell and the rotation number.

3.2. Recurrence Properties of the Sine Circle Map

As a prototype model of non-uniform quasi-periodic motion, we investigate the recurrence times properties of the well-known sine circle map[20]

$$x_{n+1} = x_n + \alpha - \frac{\beta}{2\pi}\sin(2\pi x_n) \qquad \text{mod } 1 \tag{77}$$

which has been widely used as a representative model of the return map in a Poincaré section in a variety of problems involving periodically forced strongly damped nonlinear oscillators, strobed at multiple periods of the external frequency. Here x_n is the phase of the forced oscillator, α is the ratio of the external forcing frequency and the frequency of the unforced oscillator, and β measures the strength of the coupling. Map (77) thus constitutes a physically relevant model on which valuable information concerning recurrence times properties can be extracted.

One of the characteristic properties of the sine circle map is the emergence and widening of resonance regions corresponding to phase-locking (the so-called Arnold tongues) in the parameter plane (α, β) as the coupling strength β increases. When $\beta > 1$ the map becomes non-invertible and the tongues start overlapping with each other, eventually leading to chaos. Between these phase-locked regions lie regions of quasi-periodic motion.

We now perform a numerical study of the recurrence behavior of the sine circle map in quasi-periodic regime.

The variables to be considered are: the first and second moment of the recurrence times as well as the values and number of the different recurrence times, as a function of the cell position and cell size. This latter dependence is a physically important aspect in prediction since the cell size represents the coarseness of a data set.

The mean recurrence time in each cell has been evaluated directly by monitoring the successive discrete recurrence times and then compared to the inverse of the cell's invariant measure (which was also numerically evaluated). Not surprisingly, an excellent agreement is found.

Now, as the non-uniformity of the invariant density typically implies a great variation among the invariant measures of the different cells, the recurrence times in each cell are expected to be highly dependent on the cell's position. Indeed, the variability of the cells's measures allows, in terms of recurrence times, the probing of different regions of the Farey branch converging to the rotation number. As typically no two cells have exactly the same invariant measure, they all experience different discrete recurrence times, or the same ones but in different proportions. As a result, the (relative) second moment of the recurrence times (which constitutes a measure of the spatial "degree of predictability") may also be expected to be a highly fluctuating quantity when spanning the phase-space partition. This is best understood by realizing that the set of values $\{\mu(C_i)/2\}_{i=1\cdots N}$ in the interval

$$I_{\varepsilon, N} = \left(\min_{i=1\cdots N} \frac{\mu(C_i)}{2}, \max_{i=1\cdots N} \frac{\mu(C_i)}{2} \right) \tag{78}$$

actually defines a pointwise interval of ε-values. Clearly, if in this ε-interval the behavior of the relative standard deviation associated to a uniform dynamics with rotation number ρ when the cell size is varied (as in Figs. 7b and 8b) displays substantial fluctuations, then there will be substantial *spatial* fluctuations of the relative variance in the non-uniform case. It should be obvious from Eqs. (45) and (46) that any variation of the cell size or, equivalently, measure, will *necessarily* imply a variation in the (relative) variance. The amplitude of these variations depends on the branch local complexity (structure), reflected by the coefficients appearing in the continued fraction expansion of the rotation number (note that there exists an algorithm to determine the continued fraction expansion of the rotation number directly from the dynamics of the circle map[21]).

Now, a randomly picked irrational number may be expected to have any degree of local complexity in its continued fraction, implying in turn that an infinite variety of behaviors in terms of recurrence times properties is to be expected in the set of all irrationals. The dependence of this spatial variability on the refinement of the partition is as follows: by increasing (decreasing) N, the ε-window generally shrinks (widens) but at the same time moves to lower (higher) values of ε, where the relative variance fluctuates faster and faster (slower and slower). All in all, this means that the relative variance will remain a spatially fluctuating quantity whatever the refinement of the partition is.

Figure 10 shows the invariant density of the variable x_n in (77) for the parameter values $\alpha = 0.73$, $\beta = 0.85$. Figures 11 and 12 illustrate how, for the same parameter values but for different N's, the discrete recurrence times depend, spatially, on the measure of the cells (that is, on the invariant density), as well as how their respective fractions vary. It is clear that the discrete recurrence times undergo sharp transitions as the measure

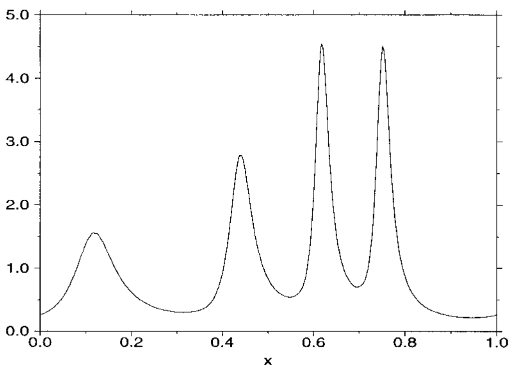

Fig. 10. Invariant density of the variable x_n in the sine circle map for parameter values ($\alpha = 0.73$, $\beta = 0.85$).

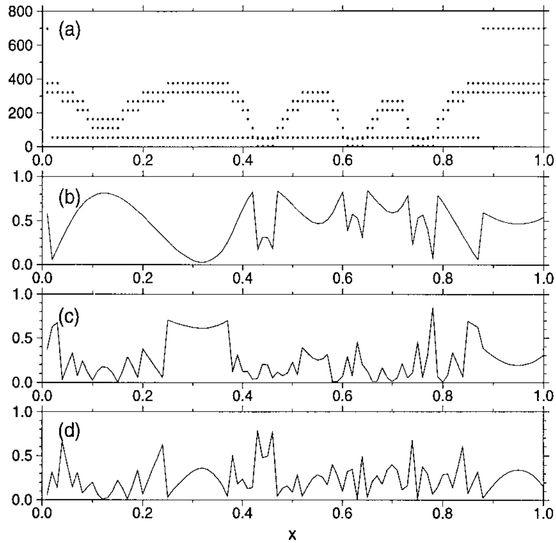

Fig. 11. Spatial distribution of recurrence times (a) and respective fractions for $N=100$ ((b): first, (c): second, (d): third), for parameter values ($\alpha=0.73$, $\beta=0.85$).

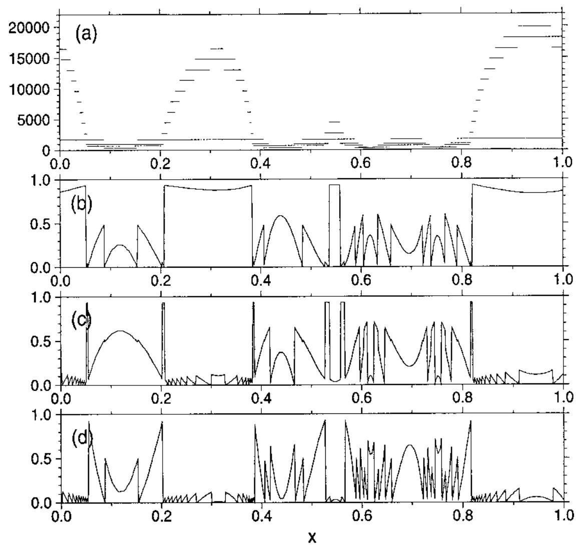

Fig. 12. Spatial distribution of recurrence times (a) and respective fractions for $N=1000$ ((b): first, (c): second, (d): third), for parameter values ($\alpha=0.73$, $\beta=0.85$).

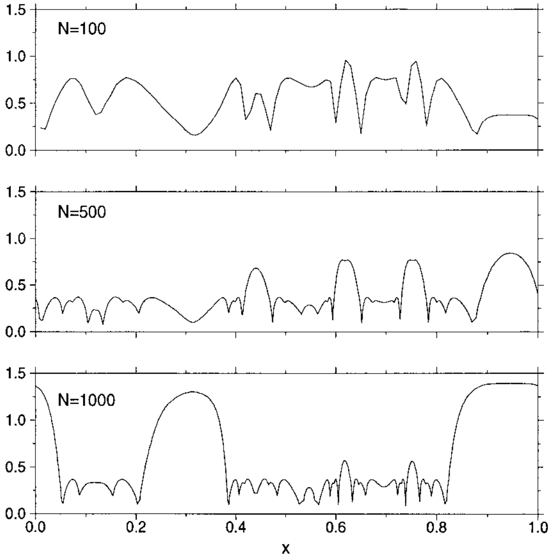

Fig. 13. Evolution of the spatial distribution of relative variance for different numbers N of cells and for the same parameter values as in Fig. 11.

of the cells reaches some specific value, with a pointwise continuous evolution of the respective fractions between two transitions (not shown), a phenomenon that is clearly reminiscent of what is observed in uniform quasi-periodic motion (uniform invariant density) when the cell size is varied.

Figure 13 illustrates how the relative variance varies for different N's, for the same parameter values. This quantity is indeed found to be highly fluctuating, both in space and as a function of the partition refinement, in agreement with the arguments advanced above. This is an important point to stress as it shows that already with rather simple dynamical systems (here, nonuniform quasi-periodic motion) the prediction of a recurrence may be rather poor and strongly dependent on the position and size of the partition cell.

4. CONCLUSIONS

In this paper we studied the recurrence times properties of the simplest form of aperiodic dynamics, the quasi-periodic motion, and their dependence on the underlying parameters. Despite its simplicity, the phenomenon of recurrence of the trajectory in a phase-space cell on the torus turned out to be quite intricate and to display a rich behavior. We derived expressions and tools that enabled us to fully understand the recurrence phenomenon in the two-dimensional case. These allowed us to determine, semi-analytically, the discrete recurrence times and their temporal succession, the mean recurrence time and the higher moments, as well as how these variables evolve in the parameter plane (ε, α). We stressed the role of the continued fraction expansion properties of the irrationals on the variability of the recurrence times. We investigated higher-dimensional quasi-periodic motions and found much more complex behaviors that also reveal a great variability in the recurrence dynamics. Unfortunately, a (semi-)analytical treatment doesn't seem to be possible in this case.

We showed that it is possible to get quantitative information about the recurrence time behavior of nonlinear systems evolving on two-dimensional tori, by casting the problem to the circle map. Evidence was produced to show that their finite-time recurrence behavior may be highly dependent on the phase-space position, the parameter values (which determine the rotation number) and the resolution of the partition. The "degree of predictability" (measured by the relative standard deviation) was related to the behavior of the Farey branch converging to the irrational rotation number, and its dependence on the cell size and position was analyzed in detail.

A major difficulty arises when higher-dimensional tori are considered, either because the forcing is higher-dimensional or because several nonlinear oscillators are coupled and possibly forced. One is then typically left with coupled circle maps, for which it is generally not possible to find a conjugacy to a pure irrational rotation although the rotation number might exist and be well defined. The above analysis then does not carry through. Of great interest would be the case of systems generating deterministic chaos where the rotation number opens up to a rotation interval or, more generally, in higher dimensions, to a rotation set[22, 23] and for which recurrence times can be expected to be statistically distributed in a much wider range, in a way closer to what happens in stochastic processes. It is not unrealistic to expect such chaotic regimes to display recurrence time properties reminiscent to what is found in quasi-periodic regime. Quasi-periodically forced (coupled) nonlinear oscillators are also of great interest as they have been shown to display strange non chaotic behavior.[24–27] The implications of strangeness with and without chaoticity on recurrence times properties are currently under investigation.

ACKNOWLEDGMENTS

The authors thank A. Zorich for pointing them out the relevance of some results obtained in the mathematical literature on interval exchange transformations, and for insightful comments on the manuscript.

M. Theunissen acknowledges a fellowship from the Fonds pour la Formation à la Recherche dans l'Industrie et dans l'Agriculture (F.R.I.A.). This work is supported, in part, by the Belgian Federal Office of Scientific, Technical and Cultural Affairs under the Poles d'Attraction Interuniversitaires program.

REFERENCES

1. H. L. Frisch, *Phys. Rev.* **104**:1–5 (1956).
2. P. C. Hemmer, L. C. Maximon, and H. Wergeland, *Phys. Rev.* **111**:689–694 (1958).
3. P. Bocchieri and A. Loinger, *Phys. Rev.* **107**:337–338 (1956).
4. H. Mayer, *Lett. Math. Phys.* **16**:139–143 (1988).
5. M. Kac, *Probability and Related Topics in Physical Sciences* (Interscience, New York, 1959).
6. V. Balakrishnan, G. Nicolis, and C. Nicolis, *J. Stat. Phys.* **86**:191–212 (1997).
7. C. Nicolis, *J. Atmos. Sci.* **55**:465–475 (1998).
8. C. Nicolis, G. Nicolis, V. Balakrishnan, and M. Theunissen, in *Lectures on Stochastic Dynamics* (Springer, Berlin, 1996).
9. V. T. Sös, *Ann. Univ. Sci. Budapest Eötvös Sect. Math.* **1**:127–134 (1958).
10. N. B. Slater, *Proc. Camb. Phil. Soc.* **63**:1115–1123 (1967).
11. J. H. Halton, *Proc. Camb. Phil. Soc.* **61**:665–670 (1965).
12. G. Lohöfer and D. Mayer, *Lett. Math. Phys.* **16**:145–149 (1988).
13. N. B. Slater, *Comp. Math.* **16**:176-183 (1964).
14. S. P. Kerckhoff, *Ergodic Theory and Dynamical Systems* **5**:257–271 (1985).
15. G. Rauzy, *Acta Arithmetica* **34**:315–328 (1979).
16. G. H. Hardy and E. M. Wright, *An Introduction to the Theory of Numbers* (Oxford University Press, Oxford, 1960).
17. L. Lorentzen and H. Waadeland, *Continued Fractions with Applications* (North Holland, 1992).
18. S. Kim and S. Ostlund, *Phys. Rev. A* **34**:3426–3434 (1986).
19. J. A. Walsh, *Int. J. Bif. Chaos* **5**:321–348 (1994).
20. H. G. Schuster, *Deterministic Chaos* (Physik Verlag, 1988).
21. H. Bruin, *Physica* **59D**:158–168 (1992).
22. P. Ashwin and J. W. Swift, *Nonlinearity* **7**:925–942 (1994).
23. M. Casdagli, *Physica* **29D**:365–386 (1988).
24. M. Ding, C. Grebogi, and E. Ott, *Phys. Rev. A* **39**:2593–2598 (1989).
25. C. Grebogi, E. Ott, S. Pelikan, and A. Yorke, *Physica* **13D**:261–268 (1984).
26. F. J. Romeiras, A. Bondeson, E. Ott, T. M. Antonsen, Jr., and C. Grebogi, *Physica* **26D**:277–294 (1987).
27. F. Romeiras and E. Ott, *Phys. Rev. A* **35**:4404–4412 (1987).